

Epitaxial Lift-Off for large area thin film III/V devices

J. J. Schermer*, P. Mulder, G. J. Bauhuis, M. M. A. J. Voncken, J. van Deelen, E. Haverkamp, and P. K. Larsen

Experimental Solid State Physics III, Institute for Molecules and Materials, Radboud University Nijmegen, Toernooiveld 1, 6525 ED Nijmegen, The Netherlands

Received 28 May 2004, revised 1 July 2004, accepted 5 July 2004

Published online 10 February 2005

PACS 81.05.Ea, 81.15.Kk, 84.60.Jt

The present work describes the study and improvement of the Epitaxial Lift-Off (ELO) technique, which is used to separate III/V device structures from their GaAs substrates. As a result the ELO method, initially able to separate millimetre sized GaAs layers with a lateral etch rate of about 0.3 mm/h, has been developed to a process capable to free entire 2" epitaxial structures from their substrates with etch rates up to 30 mm/h. It is shown that with the right deposition and ELO strategy, the thin-film III/V structures can be adequately processed on both sides. In this way semi-transparent, bifacial solar cells on glass were produced with a total area efficiency in excess of 20% upon front side illumination and more than 15% upon back side illumination. The cell characteristics indicate that, once the thin film processing has been optimized, ELO cells require a significantly thinner base layer than regular III/V cells on a GaAs substrate and at the same time have the potential to reach a higher efficiency.

© 2005 WILEY-VCH Verlag GmbH & Co. KGaA, Weinheim

1 Introduction

The Epitaxial Lift-Off (ELO) technique, allows for the separation of a III/V device structure from its GaAs substrate using selective wet etching of a thin $\text{Al}_x\text{Ga}_{1-x}\text{As}$ ($x > 0.6$) release layer using an aqueous HF solution [1–5]. The thin, single crystal films obtained by the ELO process can be cemented or Van der Waals bonded on arbitrary flat carriers for further processing [6, 7]. The fact that these carriers can be selected on the basis of their material properties rather than crystal growth demands opens the way for the development of new device structures. Owing to the large selectivity ($>10^6$) of the HF solution for AlGaAs over GaAs [8], the original substrate is not affected and can be reused [7], which results in a significant cost reduction of the III/V devices. This is most important for intrinsically large area, thus expensive, devices like high efficiency III/V solar cells [9–12].

In 1978 the first attempts were described to separate devices from their substrates using the extreme selectivity of an aqueous HF solution for AlGaAs over GaAs [1]. A wax layer was applied to support the circa 30 μm thick fragile films during the process. After this study the method, at that time referred to as 'Peeled Film Technology', was abandoned for a long time because the lateral etch rate through the applied 5 μm thick release layer was too low to be of any practical use. Almost a decade later, it was noted that if the film structures have a thickness in the range of a few micrometers, the tension induced by the wax support layer caused the III/V films to curl up with a radius of curvature R as they became undercut [2]. Although the actual etch mechanism remained unclear, this was concluded to be beneficial for removal of the etch products during the process, now referred to as Epitaxial Lift-Off technique. As a result the lateral etch rate V_e of the AlGaAs release layer with a typical thickness h in the 10–100 nm range

* Corresponding author: e-mail: johns@sci.kun.nl, Phone: +31 24 365 34 36

increased to about 0.3 mm/h [6]. Using this process many GaAs but also InP based devices such as photodiodes [13, 14], LEDs [15, 16], LASERS [17, 18], HEMTs [19] and FETs [20] transferred to silicon, sapphire and glass plates were demonstrated. In addition ELO devices were directly combined with glass and Lithium Niobate wave guides [21, 22], quartz based structures [23] and silicon integrated receiver or driver circuits [24, 25].

However, the process suffered from some severe limitations. First of all the etch rate was still fairly low. As a result the demonstrated devices were generally limited to several millimetres in size. ELO was typically performed by preparing the samples with wax and submerging them in the HF solution until the thin films were found floating in the solution after several hours up to several days. Secondly the tension induced by the wax could not be controlled well, which made it difficult to investigate the etch mechanism and optimize the process parameters. For industrial utilisation it is essential to obtain a better control over the technique so that the process can be optimized in order to allow for the separation of large area devices at sufficiently high etch rates without the loss of device quality. In the present work the improvements of the process in terms of sample size, etch rate and solar cell device quality which took place at the Radboud University Nijmegen are described.

2 Experimental

All epitaxial layer structures were grown by low pressure metal organic vapour phase epitaxy (MOVPE) on 2 inch diameter (100) GaAs wafers with a misorientation of 2° towards [110]. Arsine and phosphine were used as group-V source gasses, trimethyl-gallium, trimethyl-indium and trimethyl-aluminium as group-III precursors. Disilane and diethyl-zinc were used for respectively n and p-type doping. Growth was performed at a temperature of 650 °C and a pressure of 20 mbar. Details of the ELO process as well as the characterisation techniques used to study the samples and devices are described in previous work [4, 5, 11, 12, 26].

3 Sample size

Since it is hard to control fragile thin-film single crystal structures, it is found necessary to mount a HF resistant temporary carrier on top of the epilayer. This carrier provides continuous support and allows for manipulation of the thin film during and after the lift-off process. Because the film needs to curl up in the process a flexible carrier is required. Rather than the tension in a wax layer to force the crevice open during the etch process, now a controllable external force can be applied to the film via the carrier (see Fig. 1).

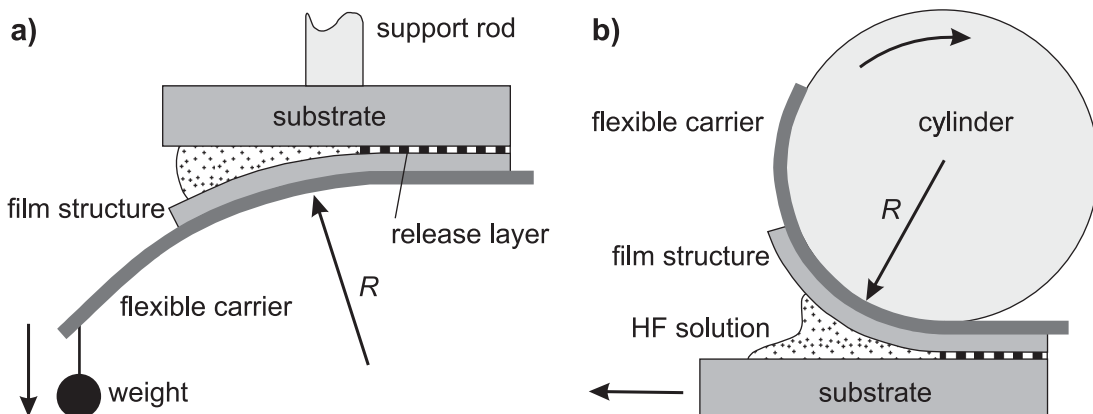


Fig. 1 Schematic representation of the ELO process. a) The weight induced ELO process, b) ELO with a stabilized radius of curvature by guiding the temporary flexible carrier over a cylinder surface.

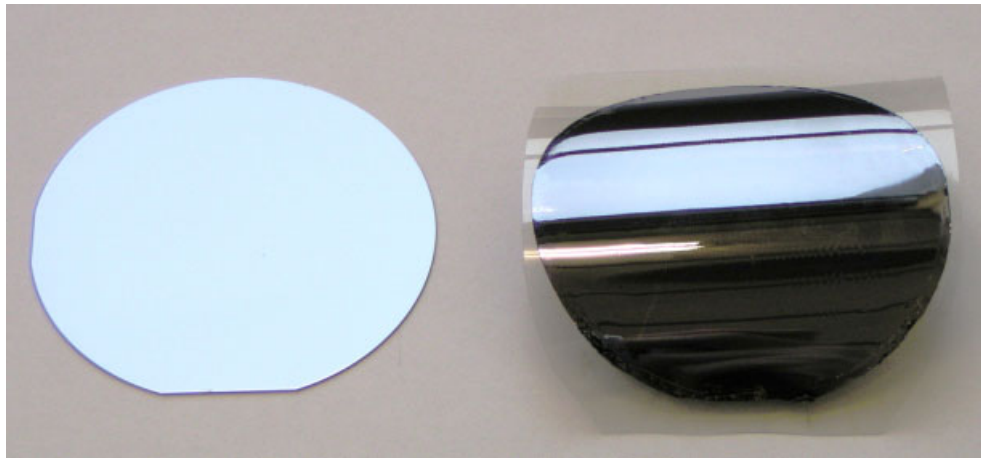


Fig. 2 (online colour at: www.pss-a.com) 1 μm thick GaAs film of 2 inch in diameter on a flexible plastic carrier (right hand side) after epitaxial lift-off from its substrate (left hand side).

At the Radboud University Nijmegen a process is developed in which the sample with the carrier is mounted upside down above the etch solution in a closed container [4, 5, 7]. A variable weight attached to the foil provides the required external force (see Fig. 1a). Due to the saturated vapour of the HF solution in the container, one droplet of etch solution positioned on the plastic foil against the edge of the sample on the side of the weight is generally sufficient to separate the epitaxial film from its substrate. A disadvantage of this configuration, also referred to as Weight Induced Epitaxial Lift-Off (WIELO), is that the flexible carrier easily bends too much, e.g. if a new droplet of HF solution needs to be applied during the process. This typically results in cracking of the epitaxial layer structure. For this reason a set-up was developed in which the slit is forced open with a constant radius of curvature by guiding the foil and the part of the film that is separated over a curved surface (see Fig. 1b).

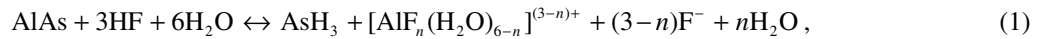
Independent of the configuration used the application of a flexible carrier proved successful for the manipulation of the films and the release of large area epitaxial layers. Figure 2 shows an 1 μm thick GaAs layer of 2 inch in diameter. At present the size of this film is determined by the maximum wafer size that can be used in our AIX200 reactor, but there seem to be no fundamental limitations to scale-up the process towards larger films.

4 Etch rate

Industrial utilization of the ELO process requires a sufficiently fast separation of the thin film devices from their substrates. The lateral etch rate of the sacrificial layer is therefore a critical factor in the process. This etch rate might be limited either by the reaction kinetics at the etch front or the diffusion of HF and reaction products towards and from this front. For both situations it is essential to know the reaction formula and stoichiometry of AIAs with an aqueous HF solution. So far, however, this reaction has not been described in literature. Therefore, research was conducted to determine the reaction products of the etch process [26]. For this purpose epitaxial AIAs layers with a thickness of 5 up to 50 μm were grown. These samples were ground up and etched with HF in a closed container. During the process gas samples were extracted from the container. After the process was completed also a sample was retrieved from the slurry formed at the bottom of the reaction vessel. Using a centrifuge the slurry was separated in its solid and aqueous compounds. This yielded a clear solution, a white powder and debris from the GaAs wafer that is virtually not etched by the HF solution.

Analyses of the gas samples extracted during the process using gas chromatography combined with various detection techniques indicated that AsH_3 and some oxygen related arsenic compound, such as As_2O_3 , are formed. Virtually no H_2 was detected, which formation was assumed in literature to derive an

expression for V_e as a function of the process parameters, i.e. the release layer thickness, the temperature T and the radius of curvature [2–4]. Nuclear magnetic resonance experiments revealed the presence of $[\text{AlF}_n(\text{H}_2\text{O})_{6-n}]^{(3-n)+}$, with $n = 0, \dots, 3$ in the solution. Scanning electron microscopy/energy dispersive spectroscopy and X-ray powder diffraction measurements on the white powder indicated the formation of an $\text{AlF}_3(\text{H}_2\text{O})_3$ compound. These results suggest a set of overall reactions given by:



with $n = 0, \dots, 3$. Under certain conditions the formation of AlF_3 which has a low solubility (white powder) might easily block the etch front if the process takes place in the ELO configuration. Additional experiments in which the AlAs samples were etched in a container with reduced oxygen levels, indicated that oxygen plays a significant role in maintaining the etch process [26]. This agrees well with the observation that in the ELO configuration (see Fig. 1) etching comes to a premature halt if the process is performed in the complete absence of oxygen. Further research is required to come to an analytical description or a computer model of the ELO process leading to a valid expression for V_e as a function of h , T and R .

A more direct approach is to determine the influence of the key parameters on the etch rate via systematic experimental research [4, 5]. These studies as performed in the WIELO configuration (see Fig. 1a) indicate that V_e increases as h decreases down to values between 3–5 nm. If h is decreased further the etch process comes to a sudden halt. V_e also increases with increasing T , but for practical reasons T is limited to 100 °C and might best be kept at a value between 50–60 °C. Finally V_e was found to increase as R is reduced. However, an increased curvature involves a higher risk of breaking the single crystal ELO films so that care should be taken with the optimisation of this parameter. Combining the results of these parameter studies and the application of a continuous flow of a 10% HF solution in our laboratory, resulted in lateral etch rates exceeding 30 mm/h.

5 Solar cell device processing

As mentioned before the cost reduction that can be obtained by the ELO process is of particular importance for intrinsically large area devices such as solar cells. Furthermore, the ability to transfer the device to an arbitrary carrier allows for the creation of new device structures. At the Radboud University Nijmegen for example a processing scheme has been developed to produce semi-transparent or bifacial III/V solar cells by transferring the device structure to a glass substrate and the application of grid contacts at both sides of the thin film (see Fig. 3).

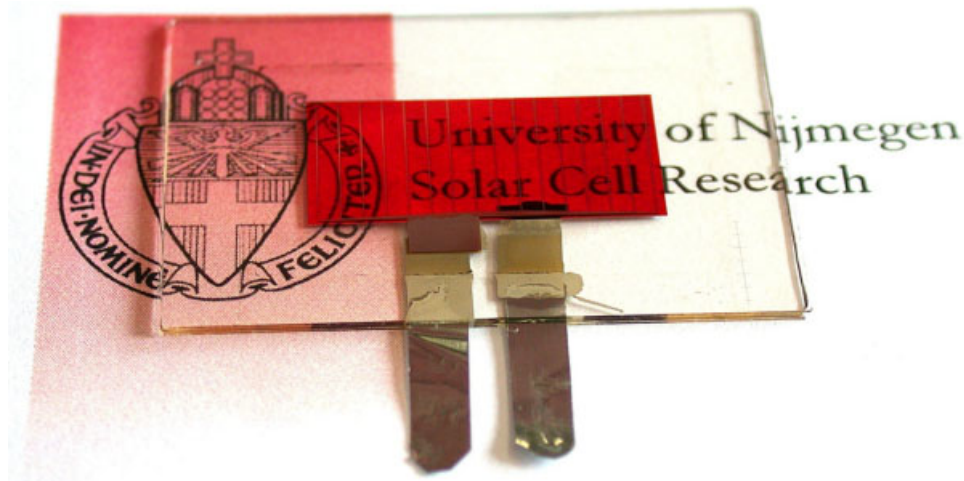


Fig. 3 (online colour at: www.pss-a.com) 1 μm thick ELO InGaP cell of 2 cm² behind a glass carrier. The cell, which has overlapping front and back grid contact patterns, is partly illuminated from the rear side to show its semi-transparency.

In this process scheme an AlAs release layer with a thickness of 5 nm is grown first, followed by the *n-on-p* cell structure with the layers in reverse order, i.e. the *n*-type layers are grown first [11]. After growth, first the *p*-type Au/Zn/Au metal rear contact is deposited by vacuum evaporation and annealed at 450 °C to ensure low contact resistivity. This rear contact might either fully cover the cell area or be a grid pattern to obtain semi-transparent or bifacial cells. Then the transient plastic support foil is attached on top of the sample to lift the thin-film structure from its GaAs substrate. After ELO the front side of the cell structure is accessible for the deposition of the *n*-type Pd/Ge contact, which only requires annealing at a relatively low temperature of 175 °C to ensure a low contact resistivity. Following metallization, the GaAs contact layer between the fingers of the grid contact is etched away and a 58 nm ZnS (refractive index $n = 2.4$) anti-reflection coating (ARC) is evaporated on top of the cell. The thin film cell is mounted behind a glass plate using optically transparent glue. The plastic foil is removed from the back side of the cell and a mesa etch process is used to define the exact cell area and provide access to the front contact. Metal tabs are connected to the front and back contacts of the cell using an electrically conductive paste. If necessary, the cell is encapsulated by a second glass plate at its rear. The result of this processing scheme applied to an 1 μm thick InGaP cell structure is shown in Fig. 3. With a bandgap of about 1.9 eV such a semi-transparent InGaP cell is a good candidate to be mechanically stacked on top of a silicon cell in order to create a dual junction solar cell.

Alternatively, a semi-transparent ELO cell might be applied as a bifacial cell. In this role the current density of the cell can be increased by illumination from both sides using a relatively cheap mirror set-up. With a bandgap of 1.4 eV GaAs is better suited than InGaP for such a single junction cell configuration. However, an optimized solar cell structure basically consists of a relatively thin highly doped emitter on top of a relatively thick base with a lower doping level. This implies that compared to front side illumination (FSI) the performance under back side illumination (BSI) will be less for such a bifacial cell. To investigate this effect a series of bifacial GaAs cells were produced with a 0.1 μm thick emitter ($n = 10^{18} \text{ cm}^{-3}$) and a base ($p = 6 \cdot 10^{17} \text{ cm}^{-3}$) with a thickness ranging from 0.25 to 2.5 μm [11]. In order to determine whether or not the ELO process influences the material quality of the devices the same layer structures were used to produce a set of regular GaAs cells, i.e. cells that remain on their GaAs substrates and have a full rather than a grid back contact. The cells produced for this comparative study are limited in size ($7 \times 8 \text{ mm}^2$) and have non-optimized metal contacts with a thickness of only 0.3 μm which cover about 5% of the cell area.

The I - V characteristics of the cells under the 1000 W/m^2 AM1.5 standard solar spectrum were determined by the use of a xenon-halogen solar simulator and a GaAs reference cell, which was calibrated at the National Renewable Energy Laboratory (NREL). The measurements of both the ELO and substrate cells yielded open circuit voltages (V_{oc}) in the 0.97–1.00 V range and fill factors (FF) between 0.76 and 0.78. The rather low FF indicates that the cells have a relatively high series resistance originating from the application of thin metal contacts. The fact that the cells have nearly identical values for V_{oc} and FF indicates that their performance is mainly determined by their short circuit current density (J_{sc}).

Figure 4 shows J_{sc} as a function of the base thickness. For the regular GaAs cells J_{sc} increases monotonically, reflecting the increased number of photons absorbed in the cell structure as the base thickness increases. The thin film cells were either subjected to FSI or BSI. Upon FSI the performance of the ELO GaAs cells differs only slightly from that of the regular GaAs cells. This indicates that the ELO process does not deteriorate the electrical and optical properties of the single crystal III/V layer structures. Compared to the processing of regular cells, the ELO cell processing scheme as described above is in a premature phase of development. This results in a slight variation in the performance of the ELO cells as obtained from identical layer structures. Solely based on the processing, J_{sc} of the ELO cells should therefore at best be equal to that of the regular cells. The fact that in some cases J_{sc} of the ELO cells is higher, results from partial reflection of the light that reaches the backside of the cell at the cell/glue interface. The reflected photons are absorbed relatively close to the *p*-*n* junction of the cell. Thus created electron-hole pairs have a higher collection probability than those created by photons that are absorbed deep in cells with larger base thicknesses. J_{sc} in ELO cells will therefore have a maximum as a function of the base thickness that is expected to surpass the maximum obtained by regular cells once the cell processing is optimized. For the cells examined in the present work J_{sc} reaches a maximum for a

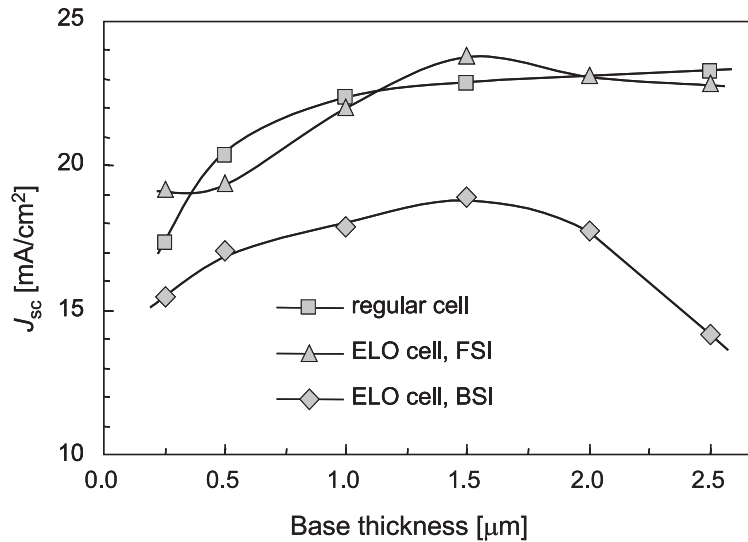


Fig. 4 Short circuit current density of bifacial ELO and regular GaAs solar cells. For the ELO cells J_{sc} for front-side illumination (FSI) as well as back-side illumination (BSI) is shown.

base thickness of 1.5 μm for FSI as well as BSI. This indicates that in order to obtain a maximum efficiency ELO cells require only half the base thickness of a regular GaAs cell which typically is 3 to 3.5 μm . Although the ELO cell was designed for FSI, J_{sc} upon rear side illumination is only 4 mA/cm² less at the optimal base thickness for the ELO cells.

Based on the above described results 2 cm² GaAs ELO cells were produced with a base thickness of 1.5 μm and an improved grid contact pattern (3% coverage). The thickness of the contacts was raised to 3 μm by electroplating. Figure 5 shows the I - V and quantum efficiency (QE) characteristics of such a bifacial ELO GaAs cell under AM1.5 conditions. Upon illumination at the front side the cell has a total area efficiency in excess of 20%. To our knowledge, this is the largest as well as the most efficient cell obtained by the application of the ELO etch technique reported in literature. Additionally the cell possesses more than 15% efficiency under BSI. From the characteristics as shown in Fig. 5 it can be de-

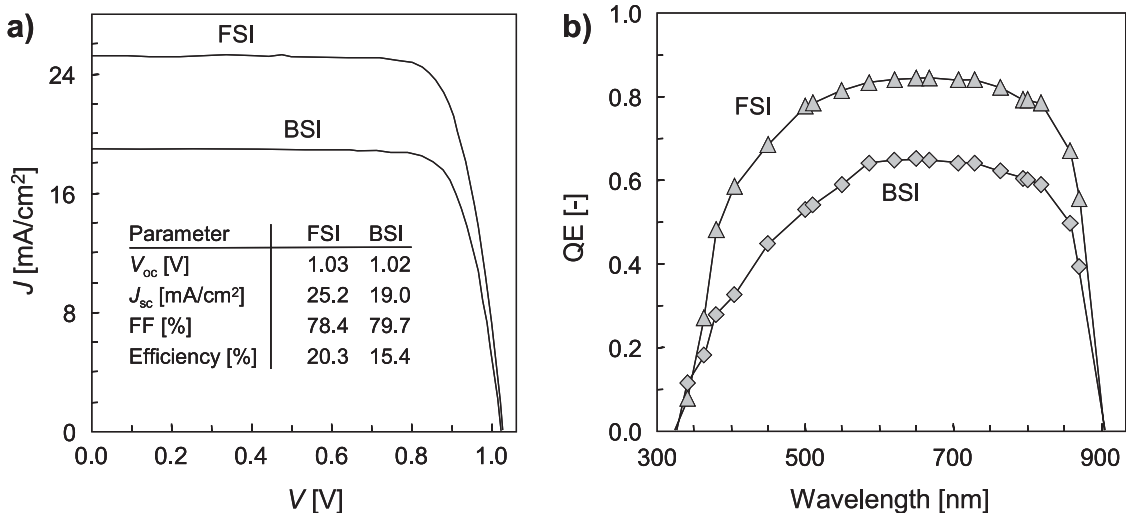


Fig. 5 a) I - V and b) quantum efficiency of a 2 cm² bifacial ELO GaAs cell with a thickness of 1.5 μm for both front-side illumination and back-side illumination.

duced how the performance of the cell should be further improved. The relatively low QE in particular for the short wavelengths show that the ARC of the cell needs to be optimized or that an additional ARC should be applied on top of the cover glass. Furthermore, the fill factors might be increased to a value well above 80%. The present values indicate the presence of a undesired series resistance which either might be related the relatively low doping level of the window layer [11] or the use of a conductive paste to connect the metal contacts to the cell. During extended thermal cycling for space application testing the latter was found to be a weak point in the present cell design [12]. Present research aims to solve these issues.

6 Conclusions

At the Radboud University Nijmegen the ELO technique has been studied and improved. Essential modifications to the original ELO method, like the use of a temporary flexible carrier and the application of an external force like a weight to open the crevice in a controlled way, have been implemented. Furthermore, the chemistry of the etch process and the influence of the different process parameters on the etch rate were examined. As a result the ELO method initially able to separate millimetre sized GaAs layers with a lateral etch rate of about 0.3 mm/h has evolved to a process capable to free entire 2" epitaxial structures from their substrates with etch rates up to 30 mm/h.

It is shown that by choosing the right deposition and ELO strategy, the thin-film III/V structures can be adequately processed on both sides. This allows for an entire range of new thin film device structures. As an example semi-transparent bifacial solar cells on glass were demonstrated in the present study. Since the cells can be mounted on an arbitrary carrier they can be optimized for different purposes. The carrier might be a light weight material for space applications, a heat conducting material for concentrator applications or any type of low bandgap cell to form a mechanically stacked tandem cell.

The high V_{oc} and FF values of the thin film cells indicate that the ELO process does not deteriorate the quality of the epitaxially grown layer structures. Resulting from reflection of light at the foreign substrate at the rear side, the ELO solar cells exhibit an enhanced collection probability of the photon induced carriers compared to regular III/V cells on a GaAs substrate. This means that, once the thin film processing has been optimized, ELO cells require a significantly thinner base layer than regular III/V cells and at the same time they might reach a higher efficiency.

Acknowledgements The authors thank the Netherlands Technology Foundation (STW) and the Netherlands Agency for Energy and the Environment (NOVEM) for financial support.

References

- [1] M. Konagai, M. Sugimoto, and K. Takahashi, *J. Cryst. Growth* **45**, 277 (1978).
- [2] E. Yablonovitch, T. Gmitter, J. P. Harbison, and R. Bhat, *Appl. Phys. Lett.* **51**, 2222 (1987).
- [3] J. Maeda, Y. Sasaki, N. Dietz, K. Shibahara, S. Yokoyama, S. Miyazaki, and M. Hirose, *Jpn. J. Appl. Phys.* **36**, 1554 (1997).
- [4] J. J. Schermer, G. J. Bauhuis, P. Mulder, W. J. Meulemeesters, E. Haverkamp, M. M. A. J. Voncken, and P. K. Larsen, *Appl. Phys. Lett.* **76**, 2131 (2000).
- [5] M. M. A. J. Voncken, J. J. Schermer, G. Maduro, G. J. Bauhuis, P. Mulder, and P. K. Larsen, *Mater. Sci. Eng. B* **95**, 242 (2002).
- [6] E. Yablonovitch, D. M. Hwang, T. J. Gmitter, L. T. Florez, and J. P. Harbison, *Appl. Phys. Lett.* **56**, 2419 (1990).
- [7] P. R. Hageman, G. J. Bauhuis, A. van Geelen, P. C. van Rijsingen, J. J. Schermer, and L. J. Giling, *IEEE Proc. 25th Photov. Specialists Conf. (Washington, 1996)*, p. 57.
- [8] X. S. Wu, L. A. Coldren, and J. L. Merz, *Electron. Lett.* **21**, 558 (1985).
- [9] F. Omnes, J.-C. Guillaume, G. Nataf, G. Jäger-Waldau, P. Vennegues, and P. Gibart, *IEEE Trans. Electron Devices* **43**, 1806 (1996).
- [10] Y. Yazawa, J. Minemura, K. Tamura, S. Watahiki, T. Kitatani, and T. Warabisako, *Sol. Energy Mater. Sol. Cells* **50**, 163 (1998).

- [11] G. J. Bauhuis, J. J. Schermer, P. Mulder, M. M. A. J. Voncken, and P. K. Larsen, *Sol. Energy Mater. Sol. Cells* **83**, 81 (2004).
- [12] J. J. Schermer, P. Mulder, G. J. Bauhuis, P. K. Larsen, G. Oomen, and E. Bongers, *Prog. Photovolt., Res. Appl.*, accepted for publication.
- [13] H. Schumacher, T. J. Gmitter, H. P. LeBlanc, R. Bhat, E. Yablonovitch, and M. A. Koza, *Electron. Lett.* **25**, 1653 (1989).
- [14] F. Kobayashi and Y. Sekiguchi, *Jpn. J. Appl. Phys.* **31**, L850 (1992).
- [15] I. Schnitzer, E. Yablonovitch, C. Caneau, T. J. Gmitter, and A. Scherer, *Appl. Phys. Lett.* **63**, 2174 (1993).
- [16] Y. Sasaki, K. Katayama, T. Koishi, K. Shibahara, S. Yokoyama, S. Miyazaki, and M. Hirose, *J. Electrochem. Soc.* **146**, 710 (1999).
- [17] E. Yablonovitch, E. Kapon, T. J. Gmitter, C. P. Yun, and R. Bhat, *IEEE Photon. Technol. Lett.* **1**, 41 (1989).
- [18] I. Pollentier, L. Buydens, P. van Daele, and P. Demeester, *IEEE Photon. Technol. Lett.* **3**, 115 (1991).
- [19] D. M. Shah, W. K. Chan, C. Caneau, T. J. Gmitter, J.-I. Song, B. P. Hong, P. F. Micelli, and F. De Rosa, *IEEE Trans. Electron Devices* **42**, 1877 (1995).
- [20] T. Morf, C. Biber, and W. Bächtold, *IEEE Trans. Electron Devices* **45**, 1407 (1998).
- [21] W. K. Chan, A. Yi-Yan, T. J. Gmitter, L. T. Florez, J. L. Jackel, D. M. Hwang, E. Yablonovitch, R. Bhat, and J. P. Harbison, *IEEE Photon. Technol. Lett.* **2**, 194 (1990).
- [22] H. Suzuki, K. Komine, Q. Huang, and K. Hohkawa, *Jpn. J. Appl. Phys.* **36**, 3109 (1997).
- [23] R. Basco, A. Prabhu, K. S. Yngvesson, and K. May Lau, *IEEE Trans. Electron Devices* **44**, 11 (1997).
- [24] A. Ersen, I. Schnitzer, E. Yablonovitch, and T. Gmitter, *Solid State Electron.* **36**, 1731 (1993).
- [25] N. M. Jokerst, M. A. Brooke, O. Vendier, S. Wilkinson, S. Fike, M. Lee, E. Twyford, J. Cross, B. Buchanan, and S. Wills, *IEEE Trans. Compon. Packag. Manuf. Technol. B* **19**, 97 (1996).
- [26] M. M. A. J. Voncken, J. J. Schermer, A. T. J. van Niftrik, G. J. Bauhuis, P. Mulder, P. K. Larsen, T. J. P. Peters, B. de Bruin, A. Klaassen, and J. J. Kelly, *J. Electrochem. Soc.* **151**, G346 (2004).